Polymer 51 (2010) 5734–5743

Contents lists available at ScienceDirect

Polymer

journal homepage: www.elsevier.com/locate/polymer

Gas permeability of cross-linked poly(ethylene-oxide) based on poly(ethylene glycol) dimethacrylate and a miscible siloxane co-monomer

Victor A. Kusuma, Gabriella Gunawan, Zachary P. Smith, Benny D. Freeman*

Center for Energy and Environmental Resources, Department of Chemical Engineering, University of Texas at Austin, Austin, TX 78758, USA

ARTICLE INFO

Article history:
Received 31 August 2010
Received in revised form
25 September 2010
Accepted 28 September 2010
Available online 7 October 2010

Keywords:
Cross-linked poly(ethylene-oxide)
SiGMA
Membrane gas separation

ABSTRACT

Pure gas permeability coefficients of a series of copolymers based on polar, hydrophilic poly(ethylene glycol) dimethacrylate, $n = 14$ (PEGDMA) and siloxane-based co-monomer, [methyl bis(trimethylsiloxy) silyl] propyl glycerol methacrylate (SiGMA) are reported. SiGMA is miscible with PEGDMA and able to form homogeneous films. SiGMA contains a bulky siloxane-based end group, which acts to increase permeability, and an −OH pendant group, which increases miscibility with polar co-monomers, such as PEGDMA. As the SiGMA content in these copolymers increases to 53 vol%, CO_2 permeability increases from 95 to 255 barrer, while CO_2/N_2 and CO_2/H_2 pure gas selectivities decrease from 58 to 20 and 6.4 to 3.2, respectively. At the same time, fractional free volume of the copolymer increases from 0.118 to 0.140. Comparisons to a similar copolymer system are made to rationalize the permeability and selectivity trends of this series of copolymers.

1. Introduction

The separation of carbon dioxide from mixtures with other gases is important for a range of applications, such as natural gas purification (CO_2 removal from mixtures with CH_4) [1], syngas purification (CO_2 separation from mixtures with H_2) [2] and post-combustion carbon capture (CO_2 removal from mixtures with N_2) [3]. In addition, membrane materials with high CO_2/O_2 selectivity are of interest in food packaging applications [4]. Ethylene-oxide based polymers have been studied extensively in recent times for some of these applications due to the favorable interaction of CO_2 with ether oxygen moieties in such materials, which promotes high CO_2/H_2, CO_2/N_2 and CO_2/O_2 selectivity [5–14].

A recent study of post-combustion carbon capture using membranes suggests that materials with higher CO_2 permeability and moderate CO_2/N_2 selectivity may be of interest for that application [3]. Along these lines, several approaches have been suggested in the literature for increasing the permeability of ethylene-oxide based polymers [15–18]. For example, Yave, Car and Peinemann blended low molar mass poly(ethylene-oxide) (PEO) with a polyether-based block copolymer, Pebax®, and observed increased CO_2 permeability and increased CO_2/H_2 selectivity [18]. Reijerkerk et al. blended Pebax® with a poly(dimethyl siloxane) (PDMS) oligomer grafted with low molecular weight PEG; an increase in CO_2 permeability was observed without a decrease in CO_2/H_2 selectivity [17]. In general, these publications report incorporation of permeability increasing siloxane-based additives, either by copolymerization, blending, grafting, or incorporation of highly mobile, low molar mass polyethers.

One challenge in modifying ethylene-oxide based polymers with, for example, permeability increasing siloxane groups is the inherent thermodynamic incompatibility of the polar ethylene-oxide based monomers and non-polar siloxane-based monomers. Recently, we proposed copolymerization of a permeability increasing siloxane-based co-monomer, 3-[tris(trimethylsiloxy)silyl] propyl acrylate (TRIS-A), with an ethylene-oxide based cross-linker, poly(ethylene glycol) diacrylate (PEGDA) (*cf.* Table 1) [15]. TRIS-A is structurally similar to components used in soft contact lenses to increase oxygen permeability [19,20]. The monomeric components used to prepare these copolymers are not miscible with one another, prompting the use of toluene, a common solvent, to permit mixing of the monomeric species prior to polymerization. Following polymerization, toluene is removed by solvent evaporation, and the resulting copolymers cannot undergo large-scale phase separation due to the covalent chemical bonds linking these inherently thermodynamically incompatible components into a cross-linked network.

Tanaka et al. proposed several monomers that have permeability increasing siloxane units but also contain structural elements designed to enhance thermodynamic compatibility with polar co-monomers used in contact lens formulations [21]. Such co-monomers can be employed to eliminate the use of solvent in making copolymers with ethylene-oxide based co-monomers. One

* Corresponding author. Tel.: +1 512 232 2803; fax: +1 512 232 2807.
E-mail address: freeman@che.utexas.edu (B.D. Freeman).

0032-3861/$ – see front matter © 2010 Elsevier Ltd. All rights reserved.
doi:10.1016/j.polymer.2010.09.069

Table 1
Chemical structures of PEGDMA, SiGMA and related materials.

Name	Structure
PEGDMA	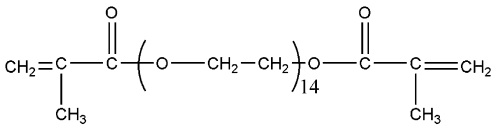
PEGDA	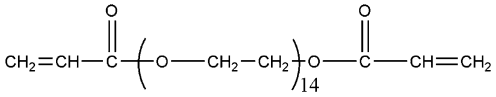
SiGMA	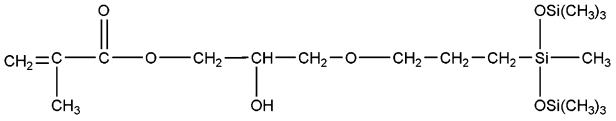
TRIS-A	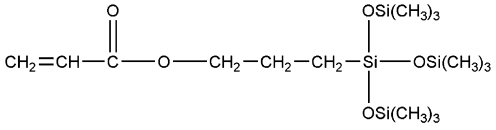
PEGMEA	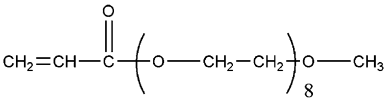

NOTE: Chemical structures of PEGDA, PEGMEA, and TRIS-A are provided for comparison.

of these compounds, [methyl bis(trimethylsiloxy)silyl] propyl glycerol methacrylate (designated "SiGMA" by Tanaka et al.), was used to prepare a series of cross-linked PEO (*i.e.*, XLPEO) copolymers in this study (*cf.* Table 1). Despite the good miscibility of SiGMA with PEGDA, PEGDA/SiGMA copolymers are visibly phase-separated due to the very different reactivity of the methacrylate and acrylate groups in SiGMA and PEGDA, respectively [22]. Hence, in this study, SiGMA was copolymerized with poly(ethylene glycol) dimethacrylate ($n = 14$) (PEGDMA), which results in visually homogeneous copolymers following UV cross-linking. CO_2, CH_4, H_2, N_2 and O_2 permeability coefficients of PEGDMA/SiGMA copolymers with varying compositions of SiGMA were determined. To assist in interpretation of the gas permeability results, physical properties such as density and glass transition temperature were also characterized.

2. Experimental methodology

2.1. Materials

Poly(ethylene glycol) dimethacrylate (PEGDMA; nominal M_w 750) was obtained from Aldrich Chemical Company (Milwaukee, WI). SiGMA ([methyl bis(trimethylsiloxy) silyl] propyl glycerol methacrylate) was obtained from Gelest, Inc. (Morrisville, PA) as SIM6481.15, (methacryloxy-hydroxy propoxy-propyl)methyl bis (trimethylsiloxy)-silane, 95% tech. grade. The UV photoinitiator, 1-hydroxyl-cyclohexyl phenyl ketone (HCPK), was obtained from Aldrich. Toluene (extra dry grade with molecular sieves, 99.85%) from Acros Organics (Geel, Belgium) was used to extract any unreacted monomers or other species not bound to the network as a result of polymerization. All reagents were used as received. All gases were obtained from Airgas Southwest Inc. (Corpus Christi, TX) with purity of at least 99.9% (except for methane: 99.0%) and were used as received.

2.2. Monomer characterization

The molecular weight and purity of PEGDMA and SiGMA were verified using ^{1}H NMR, ^{13}C NMR and mass spectrometry. The experimental details are furnished in a separate Supplementary section.

2.3. Film preparation

PEGDMA and SiGMA monomers were mixed directly at the desired proportions using mechanical stirring with 0.1 wt% HCPK photoinitiator. These components were completely miscible. After mixing, these mixtures were sandwiched between parallel quartz plates, separated by spacers of desired thicknesses, and exposed to 312 nm UV light at 3 mW/cm^2 in a UV cross-linking chamber (Spectrolinker XL-1000, Spectronics Corporation, Westbury, NY) to produce films with uniform thickness. This method was previously applied to polymerize acrylate-based monomers [7,12,13]. Due to lower reactivity of the methacrylate group [23], longer irradiation time was necessary to achieve essentially complete conversion of the methacrylate group. The minimum irradiation time, 270 s, was established by monitoring conversion of methacrylate group using FTIR-ATR (see below) and was sufficient for all mixtures with varying PEGDMA/SiGMA compositions.

Toluene was used to extract any sol after UV-irradiation and FTIR-ATR analysis. The films were placed in a sealed mason jar full of toluene for 5 days at ambient conditions (100 ml for 3 g of film),

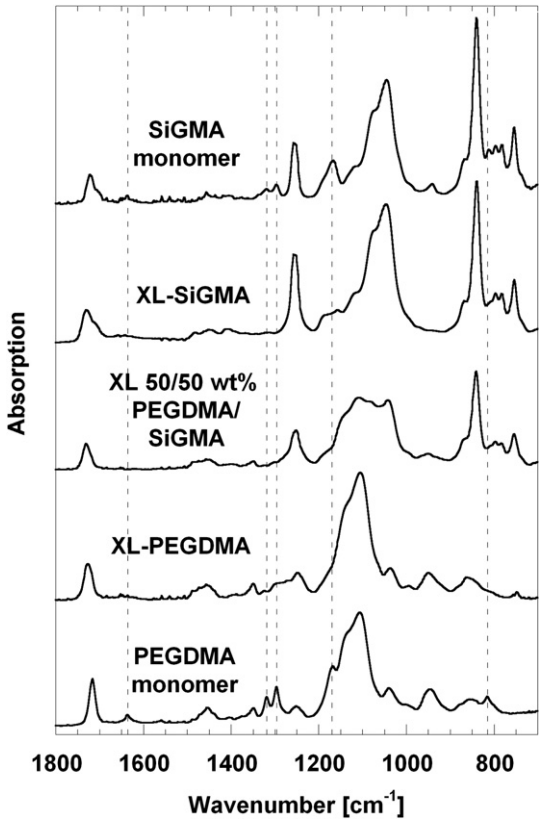

Fig. 1. FTIR-ATR spectra of PEGDMA and SiGMA monomers and polymers prepared from 100/0, 50/50 and 0/100 wt% PEGDMA/SiGMA. All polymers were extracted using toluene and air-dried prior to analysis. The spectra have been displaced vertically for clarity. Characteristic peaks for methacrylate groups are denoted by dashed line.

shaken daily without changing the toluene. The resulting transparent films were fairly fragile. Therefore, upon removal from toluene after extraction, the films were dried slowly at ambient conditions under a glass petri dish to slow the toluene evaporation rate. The typical film yield based on monomer mass is greater than 98%, indicating that the sol fraction is not significant; thus, the polymer composition is assumed to be equal to the monomer composition in the pre-polymer mixture. All compositions reported in this study are based on PEGDA/SiGMA concentrations in the pre-polymer mixtures. Dry film thicknesses were determined to within ±0.5 μm using a low force digital micrometer (Litematic VL-50A series 318, Mitutoyo Corp., Japan). The films produced were typically between 350 and 600 μm thick.

2.4. Fourier transform infrared spectroscopy

Fourier transform infrared spectroscopy was performed using a Thermo-Nicolet (Madison, WI) Nexus 470 spectrometer with attenuated total reflection (ATR) accessory. Each spectrum was averaged over 128 scans at a resolution of 4 cm^{-1}. Indicators for the disappearance of methacrylic double bonds were the peak at 1640 cm^{-1} (ascribed to C=C stretching) and at 820 cm^{-1} (H_2C = twisting) [22,24]. The paired peaks at 1330 and 1300 cm^{-1}, and at 1170 cm^{-1}, all ascribed to methacrylic C–O–C stretching vibrations [24], also disappeared after polymerization. Representative FTIR-ATR spectra of the PEGDMA/SiGMA copolymers are presented in Fig. 1.

2.5. Density measurement

Dry polymer film density was calculated based on Archimedes' principle using a Mettler Toledo (Switzerland) density determination kit for a Mettler Toledo analytical balance model AG204. This method compared the mass of dry polymer film to its mass in an auxiliary liquid that had no significant uptake in the polymer. PEGDMA/SiGMA copolymers, like the PEGDA/TRIS-A copolymers reported previously, were amphiphilic, so the auxiliary liquid chosen was a perfluorinated alkane, 3M Fluorinert™ FC-77 (obtained from Acros Organics) [15]. The densities of the PEGDMA/SiGMA copolymers in this study were estimated based on the FC-77 density value reported previously (*i.e.*, 1.765 ± 0.001 g/cm^3 at 23 °C). The effect of water vapor absorption in the polymer film was minimized by degassing the films in a vacuum oven at ambient temperature overnight, after which the chamber was filled with dry nitrogen. The subsequent re-sorption of water vapor into the polymer films, between the purge and measurement times, was determined to be negligible within the uncertainty of the experiment.

2.6. Thermal analysis

Differential scanning calorimetry (DSC) was used to determine thermal transitions of the PEGDMA/SiGMA copolymers in this study. The instrument is a TA Instruments (New Castle, DE) Q100 DSC. Samples (10–15 mg) were initially heated to 150 °C, quenched to −90 °C, and then scanned twice between these two temperatures at 10 °C/min under dry N_2 purge flow. The glass transition temperature (T_g) was taken as the midpoint of the heat capacity step

Table 2
Representative properties of cross-linked PEGDA and PEGDMA.

Properties		XL-PEGDA [12]	DM14 [28]	XL-PEGDMA (this study)
Density [g/cm^3]		1.190 ± 0.004	1.180	1.180 ± 0.004
FFV		0.120 ± 0.003	0.118[a]	0.118 ± 0.003
T_g [°C]		−37	−42	−37
Infinite dilution pure gas permeability [barrer] at 35 °C[b]	CO_2	110 ± 6	45 (25 °C); 107 (50 °C)	95 ± 5
	H_2	15 ± 0.8	–	15 ± 0.7
	CH_4	5.5 ± 0.3	–	4.8 ± 0.3
	O_2	5.1 ± 0.3	–	4.7 ± 0.3
	N_2	1.9 ± 0.1	0.7 (25 °C); 2.8 (50 °C)	1.6 ± 0.1
Pure gas selectivity	CO_2/H_2	6.9 ± 0.6	–	6.4 ± 0.5
	CO_2/CH_4	19 ± 2	–	20 ± 2
	CO_2/O_2	21 ± 2	–	20 ± 2
	CO_2/N_2	56 ± 5	68 (25 °C); 38 (50 °C)	58 ± 5
	O_2/N_2	2.7 ± 0.3	–	2.9 ± 0.3

[a] Fractional free volume of DM14 is re-calculated from density using the occupied volume (v_0) parameters in this study instead of those in Ref. [28].
[b] For DM14, permeability values are for an upstream pressure of 98 kPa (*i.e.*, 1 atm) at the temperatures specified in table.

change that appeared in the second heating scan. All samples exhibited no crystallization peaks, so these materials are amorphous, as expected.

2.7. Gas permeation measurement

Pure gas permeability was experimentally determined by measuring steady state gas flux through a film of known thickness under a fixed pressure difference [25]:

$$P_A \equiv \frac{N_A \cdot l}{p_2 - p_1} \quad (1)$$

where P_A is the permeability coefficient of the polymer to gas A, N_A is the steady state flux of gas A, l is the film thickness, p_2 and p_1 are the upstream and downstream pressures of gas A, respectively. Permeability coefficients in this study are reported in the customary units of *barrer*, where 1 barrer $= 10^{-10}$ cm^3 (STP) cm/(cm^2 s cmHg). The steady state gas flux is determined by measuring the rate of pressure increase in a pre-evacuated downstream vessel of known volume. Film area was defined by masking a sample with impermeable aluminum tape (Nashua 324A from Covalence Adhesives, Franklin, MA) that was glued using epoxy (Devcon 5 Minute® epoxy, Danvers, MA) to the upstream face of the film. The upstream gas pressures are between 3 and 10 atm. At the temperature of the experiment, 35 °C, all gases in this study are considered to behave ideally. Since the experimental setup gives the condition where $p_2 >> p_1$, p_1 was considered zero in the calculations.

3. Results and discussion

3.1. Monomer and cross-linker characterization

The number average molecular weight of PEGDMA by ^{1}H NMR analysis was found to be 757 Da, which is consistent with the supplier's specification of ~750 Da. MALDI-MS analysis further reveals that PEGDMA is relatively monodisperse, with polydispersity index of 1.02 around number average molecular weight of 860 Da. ^{1}H NMR, ^{13}C NMR and mass spectrometry analysis of SiGMA confirmed the molecular structure of this monomer and indicated the presence of some impurities. Full analysis of this cross-linker and monomer are given in a Supplementary section.

3.2. Physical characteristics of PEGDMA/SiGMA copolymers

The physical properties of UV cross-linked PEGDA (XL-PEGDA), which was characterized earlier [7,12,13,26,27], are compared with those of XL-PEGDMA in Table 2. Plasma-polymerized XL-PEGDMA for CO_2/N_2 separation was studied by Hirayama et al. [28]; the properties of this polymer (designated DM14 in Ref. [28]) are also tabulated. The use of methacrylate instead of acrylate as the polymer backbone is expected to reduce the torsional mobility of the cross-linked network, leading to increased T_g of the methacrylate-based network [23]. In practice, this effect is minimal because the physical properties of both rubbery cross-linked polymers appear to be dominated by the flexible ethylene-oxide chains, as evidenced by their similar glass transition temperatures and fractional free volumes. Because gas diffusivity in a polymer is typically strongly influenced by chain stiffness and fractional free volume [12,13], it is not surprising that the gas transport properties of XL-PEGDA and XL-PEGDMA are also similar to each other. Further comparisons of PEGDMA/SiGMA with previously-studied PEGDA copolymer systems, *e.g.* PEGDA/TRIS-A, can thus be made with minimal regards to the reactive monomer groups in the pre-polymer solution, viz. methacrylate vs. acrylate.

Fig. 2a presents the DSC scans of PEGDMA/SiGMA copolymers. A single glass transition event is observed in all copolymers studied, suggesting that the PEGDMA and SiGMA mixtures are homogeneous, resulting from random polymerization of these monomers. Addition of SiGMA qualitatively results in a slight broadening of glass transition, a reduction in the magnitude in the heat capacity change at the glass transition, and small changes in glass transition temperature. A similar broadening effect was previously shown and quantified using DMTA for the PEGDA/TRIS-A copolymers, and it was attributed to the increasing heterogeneity of the network, with increasing TRIS-A content, due to the different chemical properties of TRIS-A and PEGDA [15]. As shown in Fig. 2b, T_g was essentially unchanged in PEGDA/TRIS-A until above 80 wt% TRIS-A,

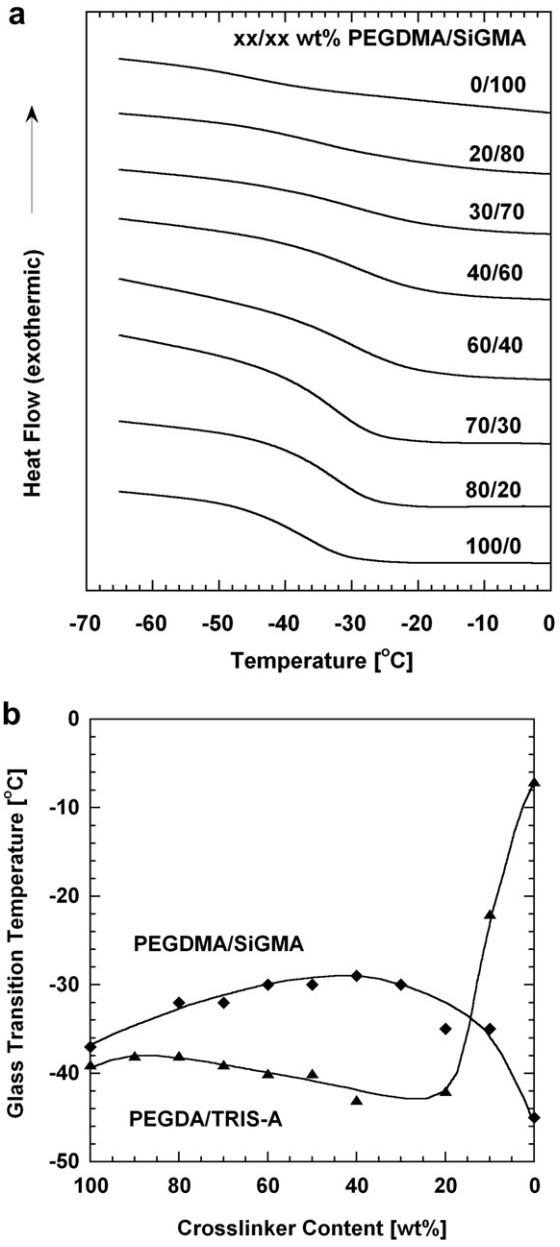

Fig. 2. a) Second scan DSC thermograms for cross-linked PEGDMA with SiGMA at different concentrations. The heating rate was 10 °C/min. The thermograms have been displaced vertically for clarity. b) Comparison of glass transition temperature (T_g) of PEGDMA/SiGMA (◆) copolymers with PEGDA/TRIS-A (▲) copolymers, as determined from the midpoint of the heat capacity step change during glass transition. The lines are drawn to guide the eye.

at which point T_g increased from −42 °C to −7 °C for the TRIS-A homopolymer. In contrast, the T_g of PEGDMA/SiGMA copolymers increases from −37 °C to −29 °C as concentration of SiGMA increases from 0 to 60 wt%. Increasing SiGMA concentration past 60 wt% decreases T_g down to −45 °C for SiGMA homopolymer. These T_g trends are also in direct contrast with PEGDA copolymers with monoacrylates containing ethylene-oxide groups (*i.e.*, chemically more compatible co-monomers), where T_g trends follow the Fox equation [6,12,13].

The unusual T_g trend of the PEGDMA/SiGMA copolymers is rationalized as follows. As shown in the previous studies, the choice of terminal functional groups on reactive monoacrylate groups in these monomers affects the T_g trend. For instance, 2-hydroxyethyl acrylate (2-HEA, with a −OH terminal group) can form hydrogen bonds with polar ether oxygens in the cross-linker and with each other. Consequently, T_g increases from −37 °C for XL-PEGDA to 14 °C for XL-2-HEA [12]. Increased compatibility of SiGMA with hydrophilic materials, as compared to TRIS and TRIS-A, is due to both reduced siloxy content and addition of an -OH side group (*cf.* Table 1). The T_g of PEGDMA/SiGMA with increasing concentration of SiGMA evolves due to the interplay between increasing −OH content, which can hydrogen bond with polar groups and would tend to increase T_g, with the reduction of overall polar group content as ether oxygen concentration decreases and non-polar siloxy group concentration increases, which would tend to decrease T_g. The polymer chains seem to be, on average, least mobile when there is an optimum concentration of −OH groups to hydrogen bond with the polar groups (ether oxygen and other −OH groups), which occurs around 40 wt% PEGDMA/60 wt% SiGMA (*i.e.*, ~5 ether oxygen per −OH moiety). The relatively small variations in chain mobility over the range of SiGMA compositions, however, likely mean that the contribution of changes in chain mobility to gas permeability would be minimal.

Fractional free volume (*FFV*) is a measure of chain packing efficiency, characterizing the amount of free space available for gas permeation in the polymer [29]. Thus, gas transport properties in a polymer are often rationalized in terms of *FFV* [30]. *FFV* is estimated from polymer density measurement as follows [29]:

$$FFV = \frac{v - v_0}{v} \quad (2)$$

where v is the specific volume of the polymer and v_0 is the specific occupied volume at 0 K, estimated by the group contribution method as 1.3 times the van der Waals volume of the chemical moieties in the polymer repeat unit. The van der Waals volume is estimated using a group contribution method described in van Krevelen [31].

Table 3 presents *FFV* values of the PEGDMA/SiGMA copolymers. Comparisons of *FFV* and density with those of PEGDA/TRIS-A copolymers are given in Fig. 3. Addition of TRIS-A to PEGDA leads to significant reductions in polymer density, which translates into increased *FFV*. A comparable increase in *FFV* is obtained upon addition of SiGMA to PEGDMA. The two monomers, TRIS-A and SiGMA, were designed with similar siloxane-based terminal groups which, due to their bulk and non-polar nature, were expected to increase the local free volume available for gas transport by opening up the largely-polar network. However, *FFV* is not a sole determinant for gas transport properties of these copolymer systems, as will be discussed in the following section.

3.3. Gas transport properties

The influence of upstream pressure on gas permeability of a representative PEGDMA/SiGMA copolymer is shown in Fig. 4. The order of permeability, $CO_2 > H_2 > CH_4 \approx O_2 > N_2$ is consistent with the order exhibited by other XLPEO copolymers and rubbery polymers in general [6,12,13,15], showing that PEGDMA/SiGMA membranes are CO_2-selective, even over small molecules such as

Table 3
Density, fractional free volume and glass transition of PEGDMA/SiGMA copolymers.

PEGDMA [wt%]	PEGDMA [vol%]	Density [g/cm^3]	*FFV*	T_g [°C] ± 1 °C
100	100	1.180 ± 0.004	0.118 ± 0.003	−37
80	78	1.148 ± 0.002	0.126 ± 0.002	−32
70	67	1.132 ± 0.001	0.130 ± 0.002	−32
60	57	1.115 ± 0.003	0.136 ± 0.003	−30
50	47	1.100 ± 0.001	0.140 ± 0.002	−30
40	37	1.086 ± 0.002	0.143 ± 0.002	−29
30	27	1.069 ± 0.004	0.149 ± 0.003	−30
20	18	1.055 ± 0.004	0.153 ± 0.003	−35
10	9	1.039 ± 0.003	0.158 ± 0.002	−35
0	0	–	–	−45

NOTE: The volume fraction of PEGDMA (φ_1) at a particular weight fraction (w_1) was estimated from the copolymer density (ρ_P) and the density of pure PEGDMA (ρ_M, *i.e.*, 1.180 g/cm^3) using the relation $\varphi_1 = \rho_P w_1/\rho_M$.

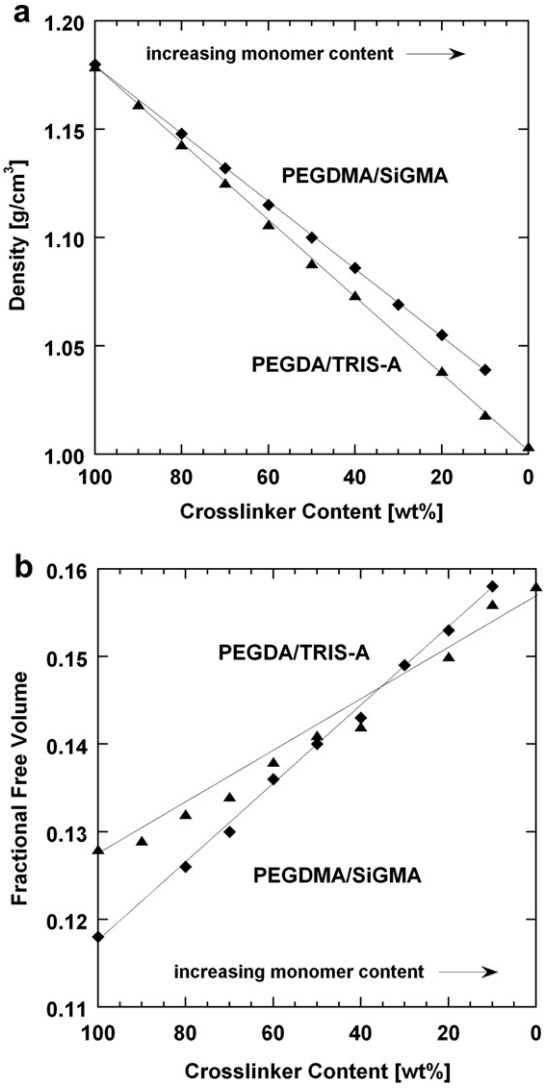

Fig. 3. a) Density and b) fractional free volume (*FFV*) of PEGDMA/SiGMA (◆) copolymers at room temperature. The results of this copolymer series are compared with those of PEGDA/TRIS-A, which were prepared with 37 wt% toluene in the pre-polymer solution (▲). The lines are drawn to guide the eye.

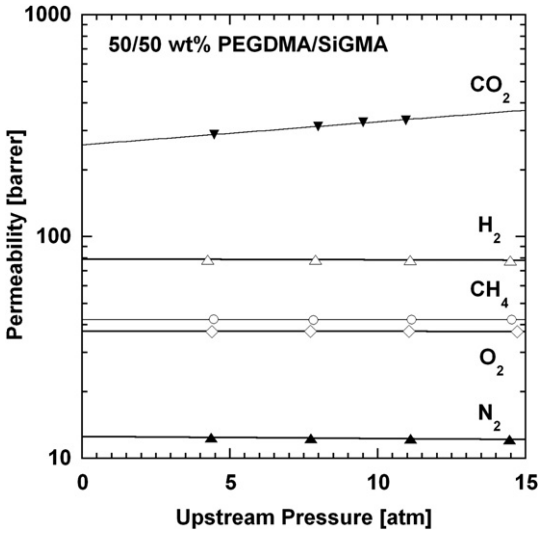

Fig. 4. Effect of upstream pressure on pure gas permeability coefficients at 35 °C in a 50/50 wt% PEGDMA/SiGMA copolymer film. The gases are ▼ CO_2, △ H_2, ○: CH_4, ◇: O_2 and ▲: N_2. The lines are drawn based on equation (3). The average uncertainty is ±6% of the permeability value.

H_2. The high permeability of CO_2 is believed to be due to favorable interactions with ethylene-oxide moieties in the cross-linker, its high condensability (as characterized by its high critical temperature) and its fairly small size (kinetic diameter of 3.325 Å [32]). CO_2 permeability increases somewhat with increasing upstream pressure, which is consistent with results in other polyether-based materials [7,12,13]. The order of the permeability coefficients of the three permanent gases (H_2, O_2 and N_2) is consistent with their sizes (2.875, 3.347 and 3.568 Å, respectively) [32]. CH_4, despite being the biggest molecule in the group (with a kinetic diameter of 3.817 Å) nevertheless has permeability on the same order as O_2, presumably due to its higher solubility [12,15].

To provide a uniform basis for comparison of intrinsic permeability coefficients, the permeability data were extrapolated to infinite dilution (*i.e.*, upstream pressure of zero) using the following empirical relationship [33]:

$$P_A = P_{A,o}[1 + m_{P,E}(p_2 - p_1)] \approx P_{A,o}(1 + m_{P,E}p_2) \quad (3)$$

where $P_{A,o}$ is the infinite dilution gas permeability and $m_{P,E}$ is an adjustable constant at a given temperature. This extrapolation is exemplified by the lines shown in Fig. 4. Using $P_{A,o}$, the broader permeability trend with addition of SiGMA to PEGDMA is shown in Fig. 5a (see also: Table 4), with side-by-side comparison to those of PEGDA/TRIS-A in Fig. 5b (taken from Ref. [15]). One interesting feature of the PEGDA/TRIS-A copolymer is the significant increase in gas permeability with increasing concentration of TRIS-A. The permeability increase is greater than those seen following the addition of comparable amount of ethylene-oxide-based comonomers such as PEGMEA (*cf.* Table 1) [10,15]. While gas

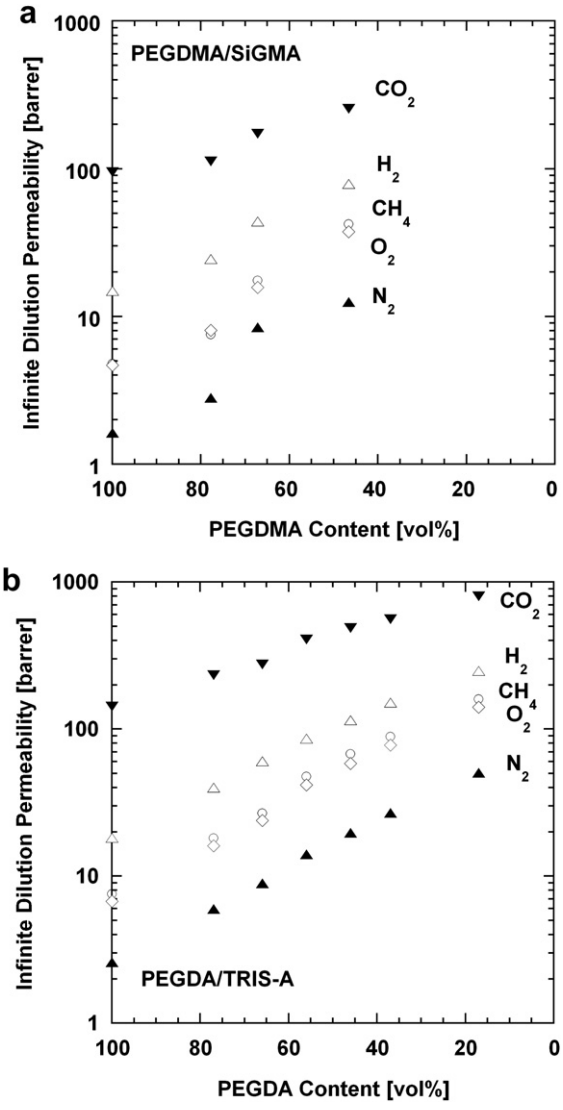

Fig. 5. Effect of SiGMA content on infinite dilution gas permeability at 35 °C. The a) PEGDMA/SiGMA series is compared with the b) PEGDA/TRIS-A series of copolymers, which is reproduced from Ref. [15]. The average uncertainty is ±6% of value. The gases are ▼ CO_2, △ H_2, ○: CH_4, ◇: O_2 and ▲: N_2.

permeability also increases with increasing SiGMA concentration in PEGDMA/SiGMA copolymers, these increases are less than those observed in the PEGDA/TRIS-A copolymer system. For instance, N_2 permeability increases from 1.6 to 13 barrer with addition of 53 vol % SiGMA to PEGDMA; over similar TRIS-A concentration range, N_2 permeability increases from 2.6 to 20 barrer in PEGDA/TRIS-A copolymers diluted with 37 wt% toluene in pre-polymer solution. Ideal CO_2/light gas selectivity (defined by the ratio of the pure gas permeability of two gas species) decreases similarly with

Table 4
Infinite dilution pure gas permeability and selectivity of PEGDMA/SiGMA copolymers at 35 °C.

PEGDMA content		Permeability [barrer]					Selectivity					
wt%	vol%	CO_2	H_2	CH_4	O_2	N_2	CO_2/H_2	CO_2/CH_4	CO_2/O_2	CO_2/N_2	O_2/N_2	H_2/N_2
100	100	95	15	4.8	4.7	1.6	6.4	20	20	58	2.8	9.1
80	78	113	24	7.5	8.1	2.8	4.6	15	14	40	2.9	8.7
60	57	173	44	18	16	8.4	3.9	9.9	11	21	1.9	5.2
50	47	255	79	42	37	13	3.2	6.0	6.8	20	3.0	6.3

NOTE: Permeability uncertainty is ±6% of value; selectivity uncertainty is ±8% of value.

increasing SiGMA or TRIS-A concentration, as shown in Fig. 6. For example, CO_2/N_2 selectivity decreases from 58 to 20 by adding 53 vol% SiGMA to PEGDMA. For comparison, CO_2/N_2 selectivity decreases from 55 to 25 for cross-linked PEGDA and cross-linked 46/54 vol% PEGDA/TRIS-A, respectively [15]. CO_2 permeability increases only from 95 to 255 barrer with addition of 53 vol% SiGMA to PEGDMA, while CO_2 permeability increases from 143 to 490 barrer with addition of 54 vol% TRIS-A.

The increase in gas permeability with increasing TRIS-A concentration was rationalized in terms of changes in gas diffusivity and solubility [15] according to the solution-diffusion model [34] (*i.e.*, $P = S \times D$). CO_2 diffusivity increased from 7×10^{-7} cm^2/s for neat XL-PEGDA to 4×10^{-6} cm^2/s for 20/80 wt% PEGDA/TRIS-A. Changes in solubility largely contributed to the selectivity trends: CO_2/light gas selectivity decreased as TRIS-A concentration increases. These trends were attributed to a significant increase in non-polar/permanent gas solubility in the polymer instead of a decrease in CO_2 solubility: for instance, as TRIS-A concentration increased from 0 to 80 wt%, CH_4 solubility increased from 0.08 to 0.33 cm^3(STP)/(cm^3 atm). This increase in solubility is likely due to incorporation of non-polar TRIS-A, which makes the chemical character of the membrane more similar to that of the non-polar penetrants. The same rationale, due to the similar character of TRIS-A and SiGMA, is likely applicable to explain the increase in gas permeability and decrease in CO_2/light gas selectivity found in the PEGDMA/SiGMA copolymers (*cf.* Fig. 6).

The comparatively lower gas permeability of the PEGDMA/SiGMA copolymers with PEGDA/TRIS-A at similar co-monomer concentrations may be due to a structural difference between SiGMA and TRIS/TRIS-A structure: the −OH side group. Previously [12], −OH terminated 2-hydroxyethyl acrylate (2-HEA) copolymers with PEGDA exhibited decreases in gas permeability, solubility and diffusivity, in contrast to PEGDA copolymers with similar co-monomers containing relatively non-polar end-groups, *i.e.*, $-OCH_3$ and $-OC_2H_5$. The hydroxyl group's ability to form hydrogen bonds with polar ether oxygen and other polar moieties in the network tends to reduce chain mobility and thus gas diffusivity. Due to the relatively non-polar nature of the mobile, bulky siloxy end-groups

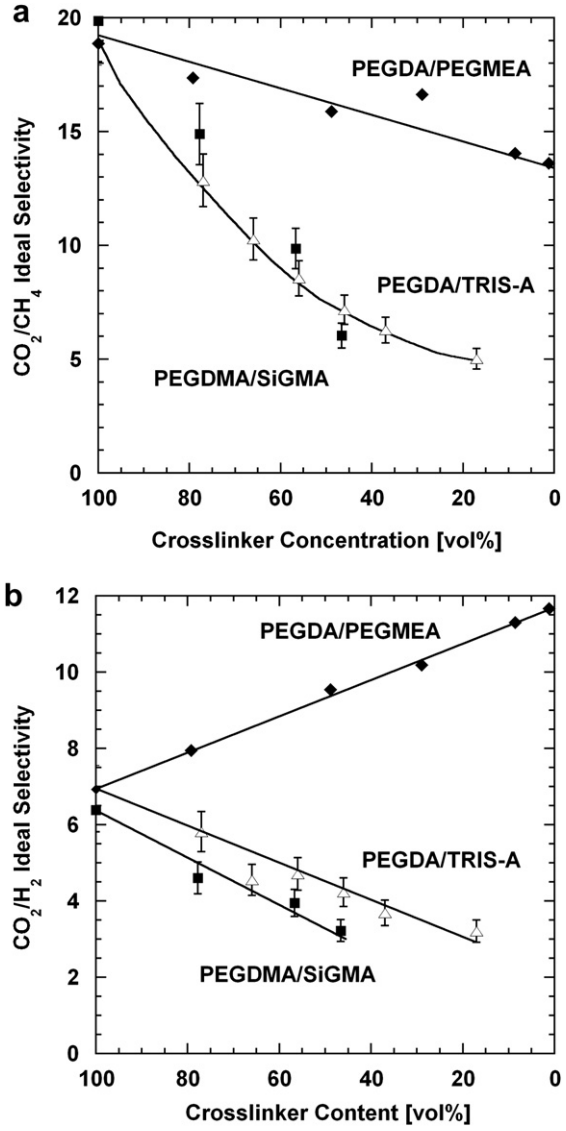

Fig. 6. Effect of co-monomer content on infinite dilution gas selectivity at 35 °C. The solid lines through the data are drawn to guide the eye. The selectivity data shown are for: a) CO_2/CH_4 and b) CO_2/H_2. Copolymers shown are PEGDMA/SiGMA (■), PEGDA/TRIS-A (△) [15] and PEGDA/PEGMEA (◆) [10].

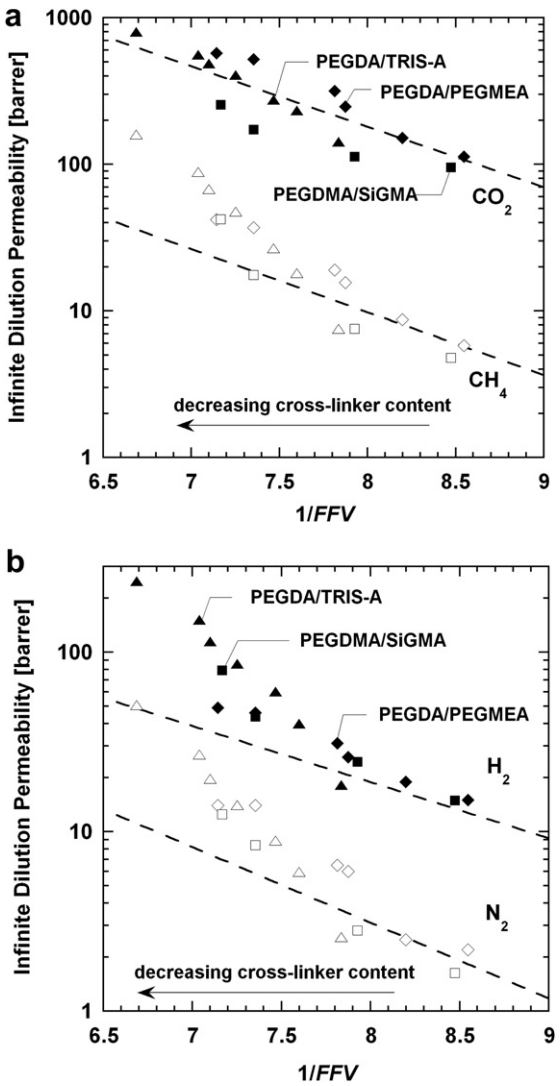

Fig. 7. Comparison between experimental and predicted infinite dilution permeability based on the free volume model (equation (5)) for: a) CO_2 and CH_4 and b) H_2 and N_2. The co-monomer content increases from right to left. Copolymers shown are PEGDMA/SiGMA (■/□), PEGDA/TRIS-A (▲/△) [15] and PEGDA/PEGMEA (◆/◇) [10]. Model lines for XL-PEGDA from Ref. [26] were displayed for comparison.

in SiGMA, gas diffusivity of the PEGDMA/SiGMA copolymers may remain high, as evidenced by the increase in permeability of all gases. However, the hydroxyl pendant groups and their propensity for hydrogen bonding nonetheless impose some restrictions on chain motion, as evidenced by the slight increase in T_g with addition of up to 63 vol% SiGMA (*cf.* Table 3). The reduced chain mobility, which tends to reduce gas diffusivity, could account for the lower gas permeability in PEGDMA/SiGMA compared to the PEGDA/TRIS-A within the composition range studied.

Lin et al. showed that the gas diffusivity in certain XLPEO materials (cross-linked PEGDA and PEGDA/PEGMEA copolymers) is a strong function of *FFV* according to the following model [6,26]:

$$D_{\text{eff}} = A_D \exp\left(-\frac{B}{FFV}\right) \tag{4}$$

where D_{eff} is the effective diffusion coefficient, and A_D and B are temperature-independent adjustable constants. The model does not always apply to other XLPEO materials containing different functional groups that interact strongly with the polymer chains [12,13]. Nevertheless, it illustrates that increasing polymer free volume often increases gas diffusivity, which, in turn, strongly influences gas permeability. As gas permeation through a dense polymeric membrane is described by the solution-diffusion mechanism, *i.e.*, $P = S \times D$, permeability is then correlated with *FFV* by:

$$P_A = S_A \times A_D \exp\left(-\frac{B}{FFV}\right) \tag{5}$$

where S_A is the solubility coefficient (ratio of gas concentration in the polymer to the pressure of the gas on the feed side of the film). Since gas solubility in XLPEO often varies weakly with chemical structure of the polymer, at least among the polymers considered to date, $S_A \times A_D$ is often consolidated as a constant, A_P.

The correlation between gas permeability and polymer *FFV* in PEGDMA/SiGMA copolymers is shown in Fig. 7, with PEGDA/TRIS-A and PEGDA/PEGMEA copolymers given for comparison. The bulky siloxane-based end-groups in TRIS-A and SiGMA lead to a more open polymer structure in networks with PEGDA or PEGDMA, and the subsequent increases in *FFV* appear to account for the corresponding increase in permeability. However, one set of adjustable constants (*i.e.*, A_P and B) cannot be applied to predict the separation performance of the various XLPEO polymers presented in Fig. 7. For instance, in the case of PEGDA/TRIS-A copolymers, the significant

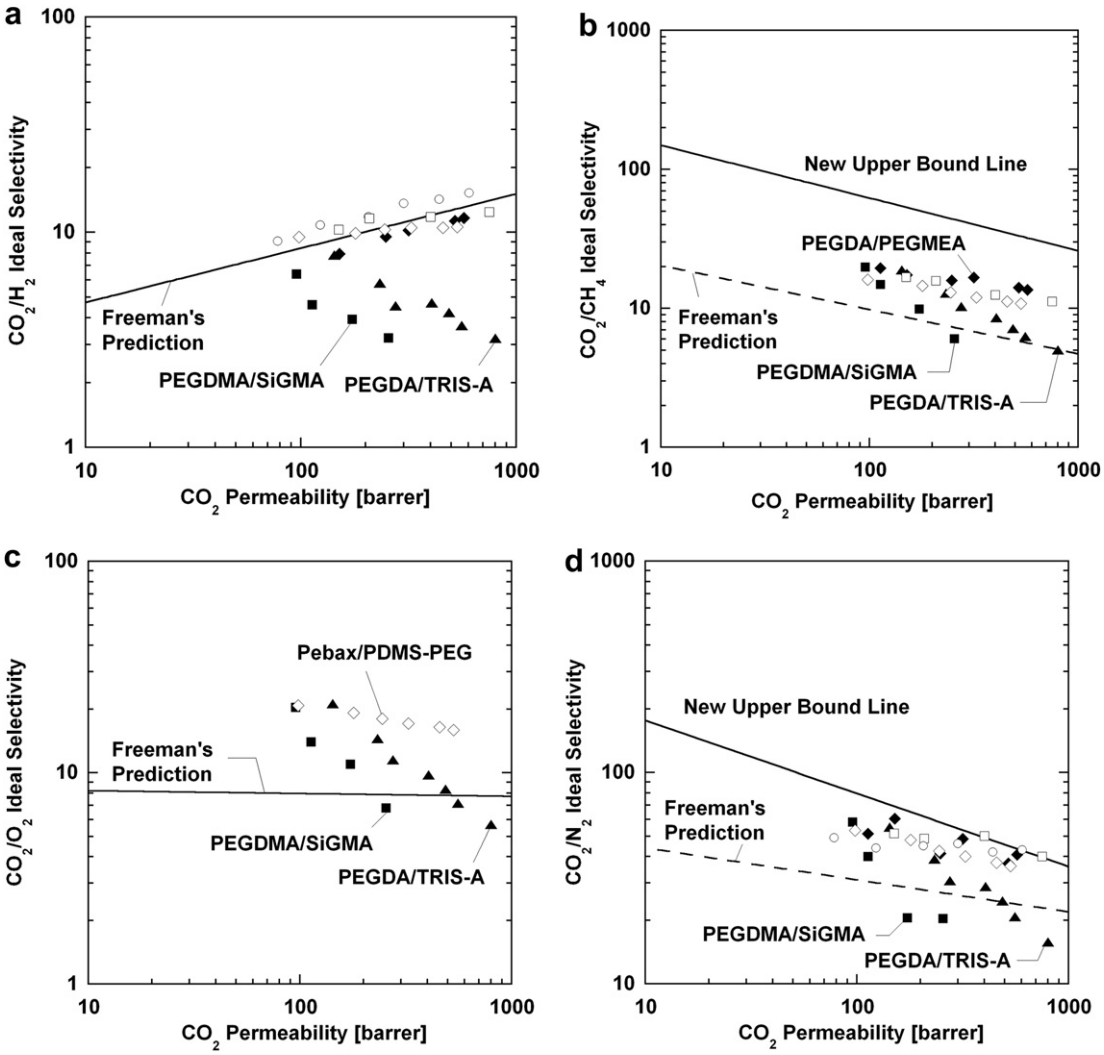

Fig. 8. Permeability/selectivity map for a) CO_2/H_2, b) CO_2/CH_4, c) CO_2/O_2 and d) CO_2/N_2, and comparison of ■: PEGDMA/SiGMA copolymers studied to ▲: PEGDA/TRIS-A [15], ◆: PEGDA/PEGMEA [10], □: Polyactive/PEG blends [38], Pebax® 1647 blends with ○: polyethylene glycol dimethyl ether [18] and with ◇: PDMS-PEG graft copolymers [17]. All data were between 30 and 35 °C and with less than 0.6 atm pressure differential (infinite dilution data provided where available). Upper bound lines were drawn based on equation (6) (labeled "Freeman's prediction") [36] and, where available, Ref. [35] (labeled "new upper bound line").

increase in non-polar gas (*e.g.*, CH_4) solubility with increasing concentration of non-polar TRIS-A leads to an increasing contribution of the solubility component to equation (5) above: *i.e.*, A_P is not constant. The changing solubility contribution effect might likewise be applicable to the PEGDMA/SiGMA copolymers. In addition to changes in chemical character of the polymers, other factors such as free volume distribution and chain mobility may contribute to the different trends shown in Fig. 7.

Gas separation performance of polymeric membranes typically exhibits a trade-off between permeability and selectivity, *i.e.*, polymers with high permeability are typically less selective [35]. The basis of this trade-off was discussed by Freeman in terms of differences in gas kinetic diameters and relative solubilities, formulated as follows [36]:

$$\ln\alpha_{A/B} = -\left[\left(\frac{d_B}{d_A}\right)^2 - 1\right]\ln P_A + \left\{\ln\left(\frac{S_A}{S_B}\right) - \left[\left(\frac{d_B}{d_A}\right)^2 - 1\right] \times \left(b - f\left(\frac{1-a}{RT}\right) - \ln S_A\right)\right\} \quad (6)$$

where $\alpha_{A/B}$ is the selectivity of gas A over gas B, with gas A taken to be the faster penetrant; d is the penetrant kinetic diameter, indicative of the penetrant size; a and b are parameters related to the correlation between diffusion front factor and activation energy [37]; f is a polymer-dependent parameter related to the average distance between polymer chains. Robeson et al. found the equation above to provide a good fit to actual experimental data for gas permeation in glassy polymers [32]. A consequence of this analysis is that the upper bound can be exceeded by changing the relative solubility of the gas pair, *e.g.*, by choosing a polymer matrix that has particular affinity to CO_2 for use in CO_2 separation applications. Rubbery polymers such as PDMS and XLPEO, which typically have high permeability and are weakly size-selective, are ideal for this approach.

The separation performance of PEGDMA/SiGMA copolymers is compared to other recent solubility-selective rubbery polymers in Fig. 8. In addition to PEGDA/TRIS-A [15] and PEGDA/PEGMEA [10], data from several recent Pebax® 1657 blends [17,18] and polyethylene oxide-poly(butylene terephthalate) (Polyactive) blends [38] are provided. CO_2/CH_4 and CO_2/N_2 are well-studied separations and common target applications for size-selective separation membranes; therefore, the upper bound lines for these separations are well established [35]. Equation (6) is employed to draw the upper bound for CO_2/O_2 separation and the so-called "reverse-selective" CO_2/H_2 separation with the following parameters: a has the universal value of 0.64, b has a value of $-\ln(10^{-4}\ cm^2/s) = 9.2$ for all rubbery polymers, f is set to zero as a first approximation, kinetic diameter values are taken from Ref. [32], and solubility parameters S are estimated from Lennard–Jones condensability parameters using $\ln S_A = -9.84 + 0.023\ K^{-1}\ (\epsilon_A/k)$, with (ϵ_A/k) taken from van Krevelen [31,36]. Critical to the success of Freeman's model is proper prediction of solubility based on the Lennard–Jones condensability parameter. Because CO_2 solubility may have not been properly predicted solely by the Lennard–Jones parameter [32], equation (6) is less successful in predicting upper bound lines involving CO_2 as a component and polymers that exhibit specific interactions with CO_2, which accounts for the difference in the two upper bound lines for CO_2/CH_4 and CO_2/N_2 (*cf.* Fig. 8b and d, respectively).

The performance trade-off between permeability and selectivity is apparent in the PEGDMA/SiGMA, like it was in the PEGDA/TRIS-A copolymer system. Both PEGDA/TRIS-A and PEGDMA/SiGMA copolymers experience significant reductions in CO_2/light gas selectivity with increasing permeability. The selectivity decrease in these solubility-selective materials is primarily the result of the changing chemical character of the copolymers with addition of the siloxane-containing co-monomers. Since CO_2 permeabilities in PEGDMA/SiGMA system are lower than those in the analogous PEGDA/TRIS-A materials, the gas separation performance of PEGDMA/SiGMA copolymers are generally further away from the upper bound than those of PEGDA/TRIS-A.

4. Conclusions

Siloxane moieties were introduced into cross-linked PEO (XLPEO) membranes via copolymerization of SiGMA, a siloxane-bearing methacrylate with chemical structure designed for compatibility with hydrophilic XLPEO precursors. Unlike TRIS-A, which required toluene as a common solvent to improve miscibility with PEGDA, SiGMA was readily miscible with PEGDMA at all concentrations, polymerizing into homogeneous films that can be used as gas separation membranes. Gas permeability increased with increasing SiGMA content in the membrane, *i.e.*, as more siloxane moieties were introduced. Addition of the relatively non-polar siloxane moieties resulted in decreasing CO_2/light gas selectivity as gas permeability increases. The increase in CO_2 permeability with addition of SiGMA to PEGDMA was less than what can be achieved by adding the same amount of TRIS-A into PEGDA. This phenomenon may be attributed to the -OH side group in SiGMA, which accounted for the slightly lower chain mobility in PEGDMA/SiGMA copolymers through hydrogen bond formation, thus presenting additional resistance to gas diffusion.

Acknowledgements

We gratefully acknowledge support by the U.S. National Science Foundation (NSF) grant CBET-0708779, the U.S. Department of Energy grant DE-FG02-02ER15362, and the Center for Layered Polymeric Systems (CLiPS), which was funded by NSF grant DMR-0423914. The authors would like to thank Ian Riddington, Aaron Rogers and Karin Keller from the Mass Spectrometry facility and Jim Wallin and Steve Sorey from the Nuclear Magnetic Resonance facility in the Department of Chemistry and Biochemistry at the University of Texas at Austin for running and interpreting the mass spectrometry and nuclear magnetic resonance spectrometry experiments.

Appendix. Supplementary data

Supplementary data associated with this article can be found, in the online version, at doi:10.1016/j.polymer.2010.09.069.

References

[1] Baker RW, Lokhandwala K. Industrial & Engineering Chemistry Research 2008;47:2109–21.
[2] Shao L, Low BT, Chung T, Greenberg AR. Journal of Membrane Science 2009;327:18–31.
[3] Merkel TC, Lin H, Wei X, Baker RW. Journal of Membrane Science 2010;359:126–39.
[4] Paul DR, Clarke R. Journal of Membrane Science 2002;208:269–83.
[5] Lin H, Freeman BD. Journal of Molecular Structure 2005;739:57–74.
[6] Lin H, Freeman BD, Kalakkunnath S, Kalika DS. Journal of Membrane Science 2007;291:131–9.
[7] Lin H, Kai T, Freeman BD, Kalakkunnath S, Kalika DS. Macromolecules 2005;38:8381–93.
[8] Lin H, Van Wagner E, Freeman BD, Toy LG, Gupta RP. Science 2006;311:639–42.
[9] Lin H, Van Wagner E, Raharjo RD, Freeman BD, Roman I. Advanced Materials 2006;18:39–44.
[10] Lin H, Van Wagner E, Swinnea J, Freeman BD, Pas SJ, Hill AJ, et al. Journal of Membrane Science 2006;276:145–61.
[11] Borns MA, Kalakkunnath S, Kalika DS, Kusuma VA, Freeman BD. Polymer 2007;48:7316–28.
[12] Kusuma VA, Freeman BD, Borns MA, Kalika DS. Journal of Membrane Science 2009;327:195–207.

[13] Kusuma VA, Matteucci S, Freeman BD, Danquah MK, Kalika DS. Journal of Membrane Science 2009;341:84–95.
[14] Richards JJ, Danquah MK, Kalakkunnath S, Kalika DS, Kusuma VA, Matteucci ST, et al. Chemical Engineering Science 2009;64:4707–18.
[15] Kusuma VA, Freeman BD, Smith SL, Heilman AL, Kalika DS. Journal of Membrane Science 2010;359:25–36.
[16] Car A, Stropnik C, Yave W, Peinemann KV. Journal of Membrane Science 2008;307:88–95.
[17] Reijerkerk SR, Knoef MH, Nijmeijer K, Wessling M. Journal of Membrane Science 2010;352:126–35.
[18] Yave W, Car A, Peinemann KV. Journal of Membrane Science 2010;350:124–9.
[19] Lai YC. Journal of Applied Polymer Science 1996;60:1193–9.
[20] Gaylord NG. U.S. Patent 3,808,178, 1974.
[21] Tanaka K, Takahashi K, Kanada M, Kanome S, Nakajima T. U.S. Patent 4,139,513, 1979.
[22] Studer K, Decker C, Beck E, Schwalm R. Progress in Organic Coatings 2003;48:101–11.
[23] Allcock HR, Lampe FW. Contemporary polymer chemistry. 2nd ed. Englewood Cliffs, NJ: Prentice-Hall; 1990.
[24] Socrates G. Infrared and Raman characteristic group frequencies. 3rd ed. Chichester: Wiley; 2001.
[25] Lin H, Freeman BD. Permeation and diffusion. In: Czichos H, Smith LE, Saito T, editors. Springer handbook of materials measurement methods. Berlin: Springer; 2006. p. 371–87.
[26] Lin H, Freeman BD. Macromolecules 2006;39:3568–80.
[27] Lin H, Freeman BD. Macromolecules 2005;38:8394–407.
[28] Hirayama Y, Kase Y, Tanihara N, Sumiyama Y, Kusuki Y, Haraya K. Journal of Membrane Science 1999;160:87–99.
[29] Lee WM. Polymer Engineering and Science 1980;20:65–9.
[30] Kumins CA, Kwei TK. Free volume and other theories. In: Crank J, Park GS, editors. Diffusion in polymers. New York: Academic Press; 1968. p. 107–40.
[31] Van Krevelen DW. Properties of polymers. 3rd ed. Amsterdam: Elsevier; 1990.
[32] Robeson LM, Freeman BD, Paul DR, Rowe BW. Journal of Membrane Science 2009;341:178–85.
[33] Stern SA, Fang S, Jobbins RM. Journal of Macromolecular Science – Physics 1971;B5:41–70.
[34] Wijmans JG, Baker RW. Journal of Membrane Science 1995;107:1–21.
[35] Robeson LM. Journal of Membrane Science 2008;320:390–400.
[36] Freeman BD. Macromolecules 1999;32:375–80.
[37] Van Amerongen GJ. Journal of Applied Physics 1946;17:972–85.
[38] Yave W, Car A, Funari SS, Nunes SP, Peinemann KV. Macromolecules 2010; 43:326–33.